第 25 卷第 10 期
2009 年 10 月

无 机 化 学 学 报
CHINESE JOURNAL OF INORGANIC CHEMISTRY

Vol.25 No.10
1797~1804

新型铜配合物[Cu(PyPt)$(NO_3)_2$]合成、结构、表征及其与 DNA 相互作用

刘 丹 周荫庄*
(首都师范大学化学系,北京 100048)

摘要:本文报道了新型铜配合物[Cu(PyPt)$(NO_3)_2$](HPyPt 是 *N*-2-吡啶基-*N*′-苯基硫脲)的合成、结构、波谱表征及其与 DNA 相互作用研究。该配合物属三斜晶系 $P\bar{1}$ 空间群,其中 a=0.761 52(15) nm,b=0.809 57(16) nm,c=1.311 3(3) nm,α=76.01(3)°,β=89.59(3)°,γ=68.24(3)°,V=0.725 5(2) nm^3,Z=2。利用荧光光谱法、紫外光谱法和粘度法初步研究了[Cu(PyPt)$(NO_3)_2$]与小牛胸腺 DNA 的相互作用,计算其与 DNA 结合常数 K_b 为 1.63×10^3 L·mol^{-1}。

关键词:铜(Ⅱ)配合物;硫脲;晶体结构;DNA
中图分类号:O614.121 **文献标识码**:A **文章编号**:1001-4861(2009)10-1797-08

Synthesis, Crystal Structure, Characterization and Studies on DNA Binding of A Novel Copper(Ⅱ) Complex [Cu(PyPt)$(NO_3)_2$]

LIU Dan ZHOU Yin-Zhuang*
(*Department of Chemistry, Capital Normal University, Beijing* 100048)

Abstract: A novel copper(Ⅱ) complex [Cu(PyPt)$(NO_3)_2$] (where HPyPt=*N*-2-Pyridyl-*N*′-Phenylthiourea ligand) had been prepared and structurally characterized, its DNA binding activity had also been investigated. The complex crystallizes in the triclinic system, space group $P\bar{1}$ with cell parameters a=0.761 52(15) nm, b=0.809 57(16) nm, c=1.311 3(3) nm, α=76.01(3)°, β=89.59(3)°, γ=68.24(3)°, V=0.725 5(2) nm^3 and Z=2. The interactions between the complex and calf thymus DNA had been investigated using fluorescent spectra, UV spectra and viscosity. The intrinsic binding constant (K_b) for complex to DNA was calculated to be 1.63×10^3 L·mol^{-1}. CCDC: 703825.

Key words: copper(Ⅱ) complex; thiourea ligand; crystal structure; DNA binding

Deoxyribonucleic acid (DNA) is the primary target molecule for most of anticancer and antiviral therapies according to the cell biology[1]. Transition metal complexes which have capable of cleaving DNA have been the focus of numerous investigations in the past two decades due to their potential use as structural probes in nucleic acids chemistry and as therapeutic agents[2~6]. Lately, various ternary copper complexes with different structural ligands exhibiting nucleolytic activities have also been studied, such as copper complexes with polymeric amino[7~12], nitrogenous base[13~17], his-dipeptide[18~20] and so on.

Our interest is in the copper(Ⅱ) complex with the ligand containing a thiourea function as well as a pyridine group as coordination sites[21~24] and further, for its possible DNA-binding activity. Recently, it is revealed that thiourea derivatives exhibit wide ranging biological activities, which including anticancer, antiviral and antibacterial, etc.

In this paper, we report the synthesis of copper(Ⅱ)

收稿日期:2009-05-18。收修改稿日期:2009-07-28。
北京市教育委员会科技发展计划面上项目(No.KM200910028011)。
*通讯联系人。E-mail:zhouyz7813@x263.net
第一作者:刘 丹,女,26 岁,硕士;研究方向:配位化学。

complex [Cu(PyPt)$(NO_3)_2$] and the corresponding ligand HPyPt[25] (where HPyPt=*N*-2-Pyridyl-*N*′-Phenylthiourea ligand), describe the structure of [Cu(PyPt)$(NO_3)_2$] and characterized it in IR, solid fluorescent spectra and cyclic voltammetric work. The DNA binding activity of the copper (Ⅱ) complex has been investigated using fluorescent spectra, UV spectra and viscosity.

1 Experimental

1.1 General procedures

All reagents used in this study are of analytical grade and were used without further purification. 2-Aminopyridine, phenylisothiocyanate, cupric nitrate trihydrate were commercially available and used without further purification. Calf thymus DNA and EB (ethidium bromide) was obtained from Sigma. The CT-DNA was dissolved in Tris-HCl buffer (5 mmol Tris-HCl +50 mmol NaCl, pH=7.4).

The infrared (IR) spectrum was recorded within the 4 000~400 cm^{-1} region on a Nicolet Impact 410 FTIR spectrometer using KBr pellets. Fluorescence Spectroscope of the complex and the interaction with EB-DNA was carried out at 293.0 K on an F-4500 FL spectrophotometer. The electrochemical measurements were done at 20 ℃ on a model 263A potentiostat/galvanostat for cyclic voltammetric work using a three electrode setup consisting of glassy carbon working, platinum wire auxiliary, and saturated calomel reference electrode. UV spectra recorded on a UV-2550 UV-Vis spectrophotometer, and UV-Vis spectrometer was employed to check DNA purity (A_{260}/A_{280}>1.80) and concentration (ε=6 600 $L\cdot mol^{-1}\cdot cm^{-1}$ at 260 nm). Viscosity was carried out on an NDJ-1 rotary viscosimeter. Melting points were determined with an SGW® X-4 microscope melting point instrument (Shanghai). X-ray diffraction was performed on a Bruker Smart 1000 CCD X-ray diffractometer.

1.2 Preparation of HPyPt

A round-bottom flask was charged with 8.0 g (89.6 mL) of 2-aminopyridine and 50 mL of absolute ethanol. To this solution phenylisothiocyanate 8.16 mL (68.8 mmol) was added using a pipette and the resulting mixture was stirred for 8 h under 78 ℃ reflux. After cooling white needles were separated from the solution[26]. The ligand was used without further purification. Yields: 75% (12.5 g). m.p. 174 ℃. Selected IR bands: 3 218($\nu_{N\text{-}H}$), 3 174($\nu_{N'\text{-}H}$), 3 037($\nu_{C\text{-}HAr}$), 1 598 ($\nu_{C=CAr}$), 1 269 ($\nu_{C=S}$), 772, 744, 693($\delta_{C\text{-}HAr}$) cm^{-1}.

1.3 Preparation of [Cu(PyPt)$(NO_3)_2$]

The title complex was prepared by a general procedure in which $Cu(NO_3)_2\cdot 3H_2O$ (484 mg, 2.0 mmol) was reacted with HPyPt (58 mg, 0.2 mmol) in 20 mL of a mixture 3∶1 (*V*/*V*) of dichloromethane-methanol. The solution was stirred for 24 h at 25 ℃. The rhombus and green crystals suitable for X-ray single crystal diffraction was obtained 7 days later. It′s quite stable in air, insoluble in most common organic solvents but easily soluble in DMF. m.p. 240 ℃.

1.4 X-ray diffraction data and crystal structure determination

A rhombus and green crystal of the title complex with dimensions 0.16 mm×0.14 mm×0.12 mm was selected for X-ray diffraction analysis. Data collection was performed on the Bruker Smart-1000 CCD area diffractometer equipped with a graphite-momochromatized Mo $K\alpha$ radiation (λ=0.071 073 nm) at 113(2) K. A total of 4 093 reflections were collected in the range of 2.80°≤θ≤25.02° for the complex, of which 2 514 (R_{int}=0.036 6) reflections were unique, and 2 212 reflections were considered as observed [$I>2\sigma(I)$]. Absorption correction was performed by the Semi-empirical from equivalents. The maximum and minimum transmission factors are 0.822 5 and 0.773 2, respectively. The structure of the complex was solved by direct method and subsequent Fourier difference techniques and refined using full-matrix least-squares procedure on F^2 with anisotropic thermal parameters for all non-hydrogen atoms (SHELXS-97 and SHELXL-97)[27]. Hydrogen atoms were added geometrically and refined with riding model position parameters and fixed isotropic thermal parameters. The final R=0.034 5, wR=0.092 1 (w=1/[$\sigma^2(F_o^2)$+(0.054 8P)^2], where P=(Max(F_o^2,0)+2F_c^2)/3).

CCDC: 703825.

1.5 DNA binding experiments

The relative binding of the complex to calf thymus (CT) DNA was studied using the fluorescence spectral

method with an ethidium bromide-bound (EB-bound) CT DNA solution in Tris-HCl NaCl buffer (pH=7.4). The concentration of CT DNA was determined from its UV absorption intensity at 260 nm with a molar extinction coefficient of 6 600 $L \cdot mol^{-1} \cdot cm^{-1}$. Fluorescence intensities at 657 nm (329 nm excitation) were measured at different complex concentrations. Addition of the complex showed a reduction in the emission intensity. The relative quenching propensity of the complex to EB-DNA was determined from the comparison of the slope of the line in the fluorescence intensity versus complex concentration plot. The quenching constant (K_D) was calculated from the Stem-Volmer equation[28] $I_0/I=1+K_D c_Q$, where I_0 and I were the fluorescence intensity in the absence and presence of quencher, c_Q was the concentration of quencher.

The UV absorption spectral method was used to determine the binding constants (K_b) of the complex using the expression $c_{DNA}/(\varepsilon_A-\varepsilon_F)=c_{DNA}/(\varepsilon_B-\varepsilon_F)+1/K_b(\varepsilon_B-\varepsilon_F)$[29], where ε_A, ε_F and ε_B are the apparent absorption coefficient, the absorption coefficient of the complex in free form, and absorption coefficient of the complex in the fully bound form, respectively. The K_b value was obtained from the $(\varepsilon_F-\varepsilon_B)/(\varepsilon_F-\varepsilon_A)$ versus $1/c_{DNA}$ plot.

Viscosity experiment was carried out with an NDJ-1 rotary viscometer in a 250 mL beaker maintained at 19±0.1 ℃. Solutions of the complexes (final concentrations ranging from 0 to 8.8×10^{-5} $mol \cdot L^{-1}$) in Tris-HCl NaCl buffer (pH=7.4) were added to a solution of calf thymus DNA (1.70×10^{-4} $mol \cdot L^{-1}$) in Tris-HCl NaCl buffer. The flow times were measured in triplicate with a stopwatch. Data were presented as $(\eta/\eta_0)^{1/3}$ versus the ratio of the complex concentration to DNA, where η is the viscosity of the DNA in the presence of the complex and η_0 is the viscosity of the DNA alone.

2　Results and discussion

2.1　Structural results

The present ligand contains two functioned groups viz., pyridine and thiourea groups (Fig.1). Interesting, sulfur in C=S bond of thiourea did not participate the coordination with copper, but form a C-S bond with C7 in benzene, forming a thiazole ring, maybe the forming of thiazole ring is the most stable structure for the complex. The bond lengths of S1-C7 and S1-C6 are 0.174 1 nm and 0.173 5 nm, shorter than general bond length of C-S (0.184 nm[30]), but longer than common bond length of C=S (0.156 nm[30]), suggesting that the bond of C-S in title complex remains part of double-bond nature.

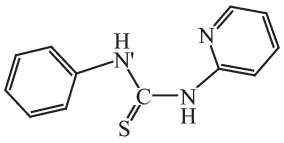

Fig.1　Structure of ligand

The title complex is characterized by single-crystal X-ray diffraction technique and the title complex crystallizes in the triclinic space group $P\bar{1}$ with a=0.761 52(15) nm, b=0.809 57(16) nm, c=1.311 3(3) nm, α=76.01(3)°, β=89.59(3)°, γ=68.24(3)°, V=0.725 5(2) nm^3 and Z=2. The summary of the crystal data, experimental details and refinement results for complex is listed in Table 1, while selected bond distances and bond angles are given in Table 2. The molecular structure of complex is shown in Fig.2. It adopts a six-coordination distorted octahedral geometry about the Cu(Ⅱ) center, the donor atoms in equatorial plane are one nitrogen atom (N1) from the pyridine of the ligand, two oxygen atoms (O4,O5) of a bidentate nitrate, one oxygen atom (O1) of another bidentate nitrate. The axial sites have coordinated one nitrogen atom (N3) from the thiourea group, one oxygen atom (O2) of the bidentate nitrate. The mean deviation from equatorial plane O1-O5-O4-N1 is 0.016 16 nm, and the distance between copper ion and the plane is 0.030 6 nm.

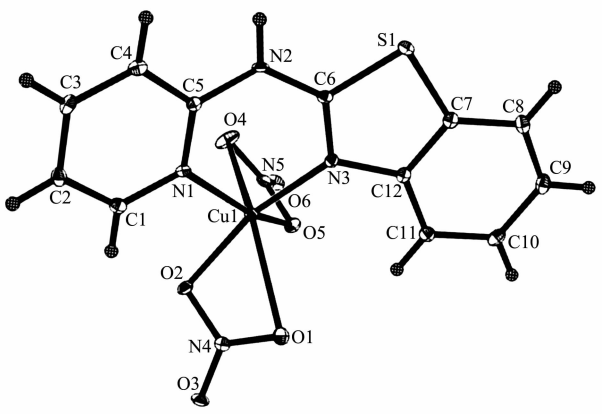

Fig.2　Molecular structure of the title complex

Table 1 Crystallographic data of title complex

Empirical formula	$CuC_{12}H_9N_5SO_6$	Z	2
Formula weight	414.84	D_c / ($Mg\cdot m^{-3}$)	1.899
Color	Green	μ (Mo $K\alpha$) / mm^{-1}	1.695
Temperature / K	113(2)	$F(000)$	418
Wavelength / nm	0.071 08	Crystal size / nm	0.16×0.14×0.12
Crystal system	Triclinic	θ range for data collection / (°)	2.80~25.02
Space group	$P\bar{1}$	$h\ k\ l$ limiting indices	−6~9, −9~9, −14~15
a / nm	0.761 52(15)	Reflections collected	4 093
b / nm	0.809 57(16)	Unique (R_{int})	0.036 6
c / nm	1.311 3(3)	GOF	1.055
α / (°)	76.01(3)	R_1, wR_2 [$I>2\sigma(I)$]	0.034 5, 0.092 1
β / (°)	89.59(3)	R_1, wR_2 (all data)	0.037 0, 0.092 9
γ / (°)	68.24(3)	Largest diff. peak and hole / ($e\cdot nm^{-3}$)	658 and −537
V / nm^3	0.725 5(2)		

Table 2 Selected bond lengths (nm) and bond angles (°) for [Cu(PyPt)(NO_3)$_2$]

Cu(1)-N(3)	0.193 3(2)	Cu(1)-N(1)	0.198 5(2)	Cu(1)-O(2)	0.199 0(2)
Cu(1)-O(5)	0.204 30(19)	Cu(1)-O(1)	0.236 7(2)	Cu(1)-O(4)	0.257 6(2)
N(3)-Cu(1)-N(1)	92.21(9)	N(3)-Cu(1)-O(4)	97.28(8)	N(3)-Cu(1)-O(5)	93.84(9)
N(3)-Cu(1)-O(1)	106.80(8)	N(3)-Cu(1)-O(2)	165.66(8)	N(1)-Cu(1)-O(4)	101.05(8)
N(1)-Cu(1)-O(5)	155.37(8)	N(1)-Cu(1)-O(1)	117.51(8)	N(1)-Cu(1)-O(2)	93.74(9)
O(2)-Cu(1)-O(5)	86.13(8)	O(2)-Cu(1)-O(1)	58.92(7)	O(5)-Cu(1)-O(1)	83.40(7)

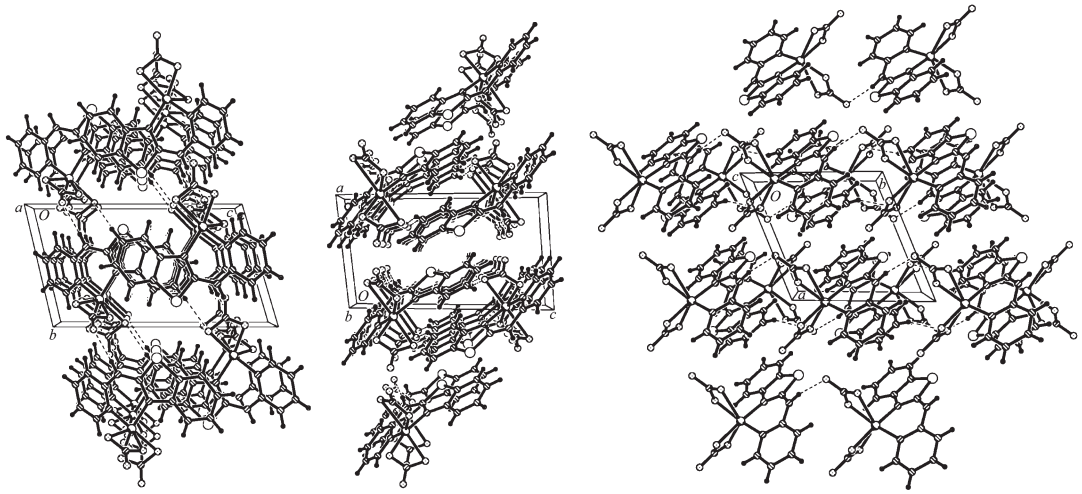

Fig.3 Packing scheme along the a, b, c axis

The benzothiazole ring of complex molecule is almost coplanar, and the dihedral angle between it and pyridine ring plane is approximately 161.3°. There are three rings around the Cu1, which are two four-membered rings consisted of bidentate nitrate and copper ions and a coordinated six-membered ring of Cu1-N3-C6-N2-C5-N1 between ligand and copper ion. The molecules of complex have regular arrangement, and adjacent molecules are central symmetry as show in Fig.3. The distance between the adjacent aromatic stacking is 0.361 7 nm, indicating the existence of π-π stacking. From packing scheme along c axis direction, it shows a typical hydrogen bonding (N2–H2···O6).

2.2 Spectral characterization

The bands in the IR region 3 174, 3 218 cm^{-1} of ligand are absent in corresponding copper(Ⅱ) complex

suggesting the deprotonation of the N′H of thiourea group due to formation of a covalent bond between the copper and thiourea nitrogen. Strong bands observed at 1 598 cm^{-1} and 1 554 cm^{-1} assigned to pyridine C=N bond stretching vibration in the ligand are shifted to lower frequency in the complex revealing the participation of the pyridine nitrogen in chelation. The band observed at 1 269 cm^{-1} assigned to C=S vibration is disappeared in the corresponding complex.

The solid-state fluorescent emission spectra for thiourea ligand HPyPt and corresponding complex [Cu(PyPt)$(NO_3)_2$] in the solid state at room temperature is shown in Fig.4 (λ_{ex}=403.0 nm). For HPyPt, the band at 459.2 nm is associated with the π-π* transition of the benzene unit, and the band at 434.2 nm is associated with the n-π* transition of the heterocyclic pyridine unit. [Cu(PyPt)$(NO_3)_2$]′s planarity is not well, so the emission intensity is weaker than ligand. Moreover, the forming of thiazole weaken the π-π* transition, the max peak at 433 nm is assigned to LMCT, the slight blue shift from 459.2 nm to 433 nm can be attributed to the ligand coordinated to metal.

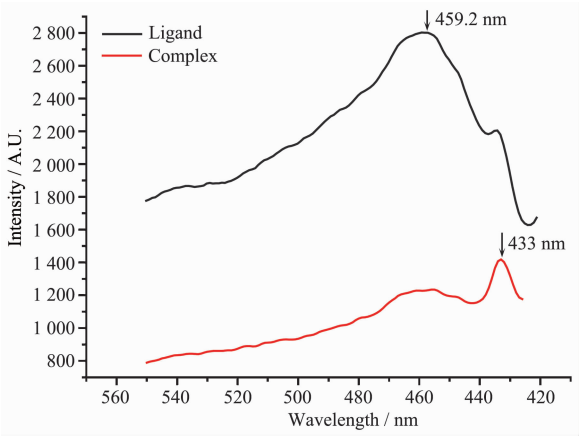

Fig.4　Solid-state emission spectra of ligand and title complex

2.3　Electrochemical property

In a DMF-1 mmol KCl buffer and with a glassy carbon working electrode, complex shows one cyclic voltammetric response attributable to the Cu^{II}/Cu^{I} couple in the 250 to 150 mV (vs SCE) potential range (Fig.5). The observation of the single redox couple, suggests a monomeric nature of the complex in solution[31~33]. When enhancing the scan rate, the peak potential difference increased, and all of them are more than 330 mV indicating the irreversible nature of the electron-transfer processes. The reduction peak current function values were found to be dependent of the scan rate (Fig.5 Inset) reveals the complex solution dominates the diffusion.

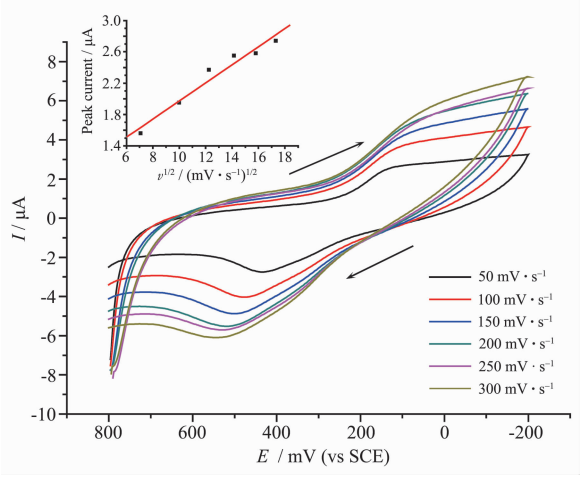

Inset: Reduction peak current vs $v^{1/2}$ (v is scan rate)

Fig.5　Cyclic voltammo gram of title complex in different scan rates

2.4　DNA binding properties

A variety of small molecules interact with double-stranded DNA, primarily through three modes: (a) electrostatic interactions with the negative charged nucleic sugar-phosphate structure, which are along the external DNA double helix and do not possess selectivity; (b) binding interactions with two grooves of DNA double helix; and (c) intercalation between the stacked base pairs of native DNA. Thus, the mode of and propensity for binding of the title complex to CT-DNA was studied with the aid of different techniques.

2.4.1　Fluorescence spectroscopic studies

Fluorescence spectral technique using the emission intensity of ethidium bromide (EB) bound to calf thymus DNA has been used to determine the binding propensity of the title complex. EB emits intense fluorescent light when it is intercalated between adjacent DNA base pairs. The addition of a second DNA-binding molecule can quench the DNA-EB adduct emission by either replacing the EB and/or by accepting the excited-state electron of the EB through photoelectron transfer mechanism[34]. Fig.6(a) shows the

emission spectra of EB bound to DNA in both the absence (the top of line) and presence of the copper(Ⅱ) complex at increasing concentrations. Addition of the complex to DNA that has been previously treated with EB causes an appreciable reduction in emission intensity, thus indicating that the complex binds to DNA. From the plot of I_0/I versus c_{DNA} (Fig.6(b)), the quenching constant (K_D) of the complex with DNA was calculated to be 0.6487.

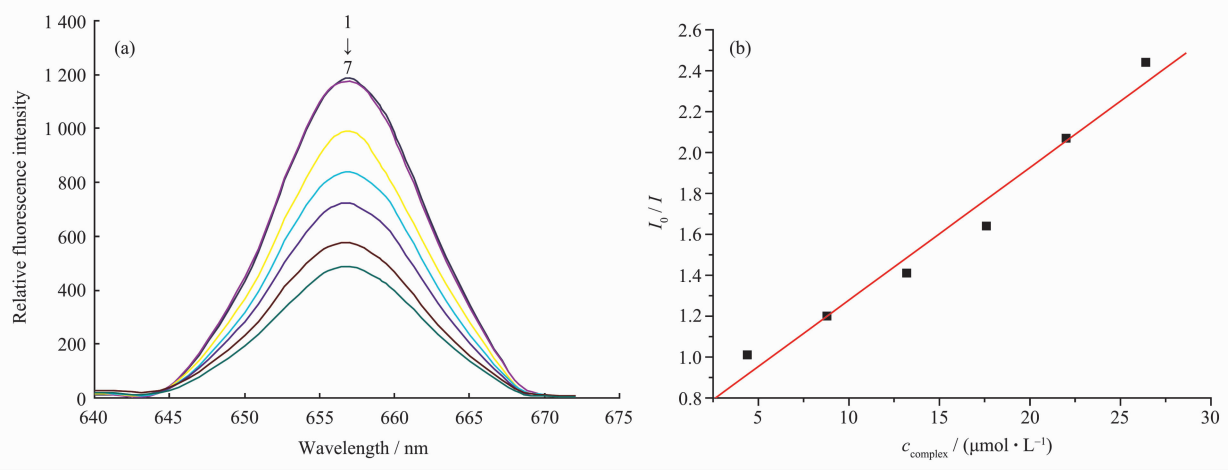

Fig.6 Change of the fluorescence intensity of DNA-EB titrated with increasing complex (a) and the plot of I_0/I vs $c_{complex}$ (b)

2.4.2 UV spectroscopic studies

DNA binding is the critical step for DNA cleavage; therefore, the potential DNA binding ability of complex was studied by UV spectroscopy by following the intensity changes of the π-π^* transition band at 317 nm. Upon addition of an increasing amount of DNA (from 0 to 4.59×10^{-5} mol·L^{-1}) to the complex (3.93×10^{-5} mol·L^{-1}), a 15% hypochromism and a slight red shift (2 nm) were observed, which suggested possible interaction such as intercalation occurred between the complex and DNA (Fig.7(a)), because intercalation would lead to hypochromism in UV absorption spectra[35,36]. From the plot of $(\varepsilon_F-\varepsilon_B)/(\varepsilon_F-\varepsilon_A)$ versus $1/c_{DNA}$ (Fig.7(b)), the intrinsic binding constant (K_b) of the complex with DNA was calculated to be 1.63×10^3 L·mol^{-1}, a value significantly lower than those obtained for typical intercalators (e.g., EB-DNA, ~10^6 L·mol^{-1}), indicating the affinity of complex for DNA is relatively low.

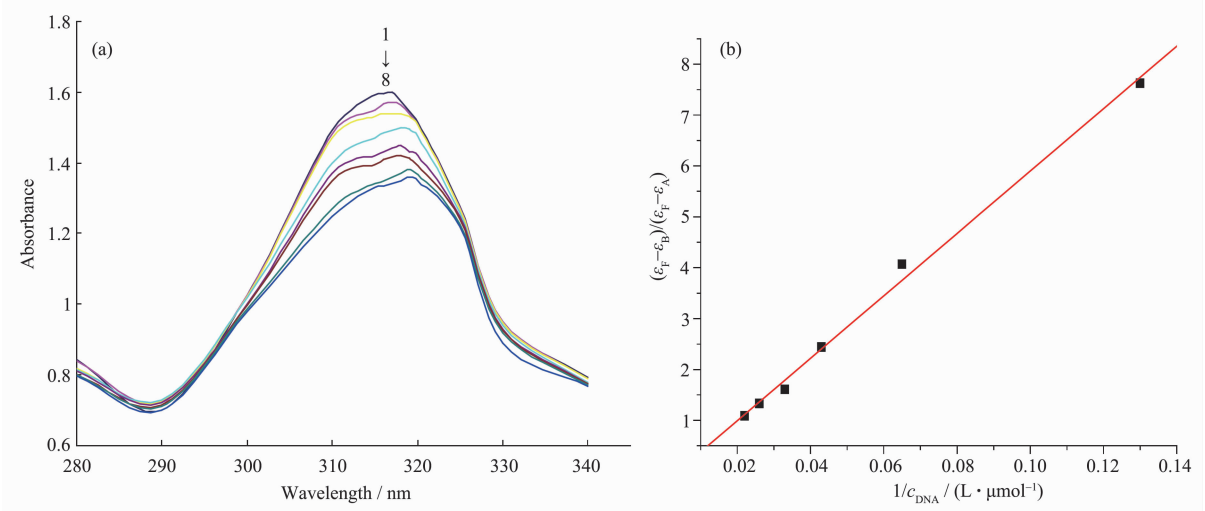

Fig.7 Change of the absorbance peak of the complex titrated with increasing DNA (a) and the plot of $(\varepsilon_F-\varepsilon_B)$ / $(\varepsilon_F-\varepsilon_A)$ vs $1/c_{DNA}$ of complex (b)

2.4.3 Viscosimetry studies

Hydrodynamic measurements that are sensitive to length changes are regarded as the least ambiguous and the most critical tests of a DNA binding model in

solution, providing reliable evidence for the DNA binding mode[34]. One classic intercalation model results in the lengthening of the DNA helix as the base pairs are separated to accommodate the binding ligand, thus leading to an increase in DNA viscosity. In contrast, complexes that bind exclusively in DNA grooves by means of partial and/or nonclassic intercalation under the same conditions typically cause either a less pronounced change (positive or negative) in DNA solution viscosity or none at all. Our result (Fig.8) reveals that the title complex has no effect on the relative viscosity of CT-DNA.

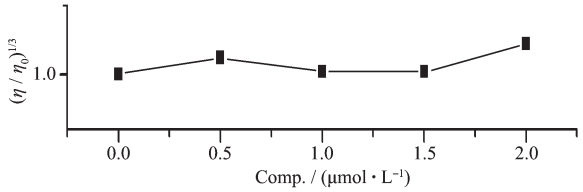

Fig.8　Effects of increasing amounts of the complex on the viscosities of DNA

These findings above indicate that the interaction does not involve a classic intercalation and that the complex probably binds either in DNA grooves or in the sugar-phosphate backbone in a partial intercalation.

3　Conclusions

In summary, a novel Cu(Ⅱ) complex [Cu(PyPt)$(NO_3)_2$] had been prepared by reacting cupric nitrate trihydrate with *N*-2-Pyridyl-*N*′-Phenylthiourea (HPyPt). The title complex was characterized by X-ray diffraction, spectroscopic (IR, solid-fluorescence) and electrochemical studies. The Cu(Ⅱ) center adopts a six-coordination distorted octahedral geometry. The structure of ligand changed when it coordinated with copper ion, and the IR and fluorescent emission spectra both reveal the phenomenon. The CV profile shows title complex a monomeric nature in solution, and it′s redox-active and irreversible cyclic voltammetric. Moreover, the interactions between the complex and CT-DNA had been investigated using fluorescent spectra, UV spectra and viscosity. Remarkably, our results show that the complex is a new piece that could bind DNA in a partial intercalation mode, but the intrinsic binding constant (K_b) is 1.63×10^3 L·mol^{-1} indicating the affinity of complex for DNA is relatively low.

References:

[1] Kang J W, Dong S Q, Lu X Q. *Bioelectrochemistry*, **2006**,**69**:58~64

[2] Sredhara A, Freed J D, Cowan J A. *J. Am. Chem. Soc.*, **2000**, **122**:8814~8824

[3] Thomas A M, Nethaji M, Chakravarty A R. *J. Inorg. Biochem.*, **2003**,**94**:171~178

[4] Reddy P A N, Nethaji M, Chakravarty A R. *Eur. J. Inorg. Chem.*, **2004**:1440~1446

[5] Scarpellini M, Neves A, Horner R. *Inorg. Chem.*, **2003**,**42**:8353~8365

[6] Kobayashi T, Tobita S, Kobayashi M et al. *J. Inorg. Biochem.*, **2007**,**101**:348~361

[7] Wang X Y, Zhang J, Li K et al. *Bioorg. Medicinal Chem.*, **2006**,**14**:6745~6751

[8] Sissi C, Mancin F, Tonellato U. *Inorg. Chem.*, **2005**,**44**:2310~2317

[9] Wang R M, He N P, Tsuchida E. *Polym. Adv. Technol.*, **2005**, **16**:638~641

[10]Hirohama T, Arii H, Chikira M. *J. Inorg. Biochem.*, **2004**,**98**:1778~1786

[11]Robertson M J, Luliis G N De, Maeder M et al. *Inorg. Chim. Acta*, **2004**,**357**:557~570

[12]An Y, Tong M L, Mao Z W, et al. *Dalton Trans.*, **2006**:2066~2071

[13]Dhar S, Chakravarty A R. *Inorg. Chem.*, **2005**,**44**:2582~2584

[14]Dhar S, Nethaji M, Chakravarty A R. *Inorg. Chem.*, **2005**,**44**:8876~8883

[15]Dhar S, Reddy P A N, Chakravarty A R. *Dalton Trans.*, **2004**:697~698

[16]Chen R, Bu X H, Yang M. *J. Inorg. Biochem.*, **2007**,**101**:412~421

[17]Thomas A M, Chakravarty A R. *J. Eur. J. Inorg. Chem.*, **2007**:822~834

[18]Reddy P R, Rao K S, Mohan S K. *Chem. Biodivers.*, **2004**, **1**:839~853

[19]Reddy P R, Rao K S, Mohan S K. *Chem. Biodivers.*, **2005**, **2**:1338~1350

[20]Reddy P R, Manjula P. *Chem. Biodivers.*, **2007**,**4**:468~480

[21]Rashdan S, Light M E, Kilburn J D. *Chem. Commun.*, **2006**:4578~4580

[22]Bayoumi H A, Shoukry E M, Mostafa M M. *Synth. React. Inorg. Met.-Org. Chem.*, **2001**,**31**(4):579~597

[23]Shoukry E M, Bayoumi H A, Mostafa M M. *Transition Met. Chem.*, **2000**,**25**:73~79

[24]Lenthall J T, Anderson K M, Steed J W. *Crystal Growth & Design*, **2007**,**7**(9):1858~862

[25]Mostafa M M, West D X. *Transition Met. Chem.*, **1983**,**8**:312~315

[26]Ferrari M B, Bisceglie F, Pelosi G. *Inorg. Chimica Acta*, **2007**,**360**:3233~3240

[27]Sheldrick G M. *SHELXS*-97 *and AHELXL*-97, *Software for Crystal Structure*, Analysis, Siemens Analytical X-ray Instruments. Inc. Madision, WI, **1997**.

[28]Mannar R. *Maueya. Eur. J. Inorg. Chem.*, **2003**:1966~1973

[29]Pyle A M, Rehmann J P, Barton J K. *J. Am. Chem. Soc.*, **1989**,**111**:3051~3058

[30]CHEN Xiao-Ming(陈小明), CAI Ji-Wen(蔡继文). *Single Crystal Structure Analysis Principles and Practices*(单晶结构分析原理与实践). Beijing: Science Press, **2003**.

[31]Thomas A M, Chakravartyet A R. *J. Eur. J. Inorg. Chem.*, **2007**:822~834

[32]Tu C, Shao Y, Guo Z J. *Inorg. Chem.*, **2004**,**43**:4761~4766

[33]Wang H S, Ju H X, Chen H Y. *Electroanalysis*, **2001**,**13**(13):1105~1109

[34]Alzuet G, Borrás J. *Inorg. Chem.*, **2007**,**46**:7178~7188

[35]Reddy P R, Rao K S, Satyanarayana B. *Tetra. Lett.*, **2006**,**47**:7311~7315

[36]Reddy P R, Manjula P. *Chem. Biodiversity*, **2007**,**4**:468~480